models can also be obtained solely on the basis of the measured effect of size on σ_N.

The size effect law in Equation 12.2.11 has also been shown to describe well the existing test data on the size effect in various brittle failures of concrete structures, in particular; (1) the diagonal shear failure of reinforced concrete beams (unprestressed or prestressed, without or with stirrups), (2) the torsional failure of concrete beams, (3) the punching shear failure of reinforced concrete slabs, (4) the pull-out failure of steel bars embedded in concrete, and (5) the ring and beam failures of plain concrete pipes (Bažant and Kim, 1984; Bažant and Cao, 1986a, b; and 1987; Bažant and Prat, 1988b; Bažant and Sener, 1987, 1988; Bažant and Kazemi, 1988, 1989). Since, in contrast to fracture specimens, concrete structures have no notches, these applications rest on two additonal hypotheses, which are normally correct for concrete structures: (1) the failure (maximum load) does not occur at crack initiation but only after a relatively long crack or crack band has developed; and (2) the shape of this crack or crack band is about the same for structures of different sizes.

It may also be noted that describing the size effect in (unnotched) structures by Equation 12.2.11 is in conflict with the classical Weibull statistical theory of size effect. However, this theory needs to be made nonlocal (cf. Sec. 13.10), and then this classical theory is found to apply only asymptotically to very small structures, while for large structures there is a transition to the LEFM size effect, similar to Equation 12.2.11 (Bažant and Xi, 1989).

Problems

12.2.1 Let $\sigma_y = F(\delta)$ = given descending function of opening δ of the equivalent elastic crack shown in Figure 12.9b. Formulate the condition that the resultant of the equivalent elastic stresses σ_y over length r_p (Fig. 12.9b) be equal to the resultant of stresses $\sigma_y = F(\delta)$ over length l_f (Fig. 12.9b). (From this condition, one can estimate the ratio of l_f to $E'G_f/f_y^2$.)

12.2.2 Rearrange Equation 12.2.11 algebraically so that Bf_t' and D_0 can be obtained from σ_N data by linear regression (Bažant, 1984).

12.3 CRACK STABILITY CRITERION AND *R* CURVE

The propagation of a crack is a problem of equilibrium and stability governed by the same laws as those for inelastic structures in general. This section will discuss the criterion of stability of a crack and explain a simple approach to handle in an equivalent elastic manner the nonlinearity of fracture caused by the existence of a nonlinear zone at the crack tip.

R Curve and Fracture Equilibrium Condition

After a crack starts from a smooth surface or a notch, the size of the fracture process grows as the crack advances. The consequence is that the energy release rate R required for crack propagation (also called the crack resistance to propagation) increases and may be considered to be a function of the distance c

of the advance of the tip of the equivalent elastic crack ($c = a - a_0$ where a = current crack length and a_0 = initial crack length or notch length). If the function $R(c)$ is known, the crack propagation may be approximately analyzed by methods of linear elastic fracture mechanics, in which constant G_f is replaced by the function $R(c)$, called the R curve (Fig. 12.12a).

To some extent, the function $R(c)$ may be approximately considered to be a fixed material property, as proposed by Irwin (1960) and Krafft, Sullivan, and Boyle (1961). It has been found, however, that the shape of the R curve depends considerably on the shape of the specimen or structure. The R curve may be assumed to be unique only for a narrow range of specimen or structure geometries. Thus, it is necessary to determine the R curve for the given geometry prior to fracture analysis. A simple method to do that, utilizing the size effect law, has been proposed by Bažant, Kim, and Pfeiffer (1986) and refined by Bažant and Kazemi (1988), and by Bažant, Gettu, and Kazemi (1989). In the analysis that follows we will assume that the R curve for the given geometry is known.

The energy that must be supplied to an elastic structure under isothermal conditions in order to produce a crack of length a is

$$\mathcal{F} = \int_0^c bR(c')\,dc' + \Pi(a) \qquad c = a - a_0 \tag{12.3.1}$$

where b = thickness of the structure and a_0 = initial crack length or notch length. $\mathcal{F}$ represents the Helmholtz free energy and Π is the total potential energy of the structure due to formation of a crack of length $c = a - a_0$. An equlibrium state of fracture occurs when $\delta\mathcal{F} = 0$, in which case neither energy needs to be supplied, nor energy is released if the crack length changes from a to $a + \delta a$. Since $\delta\mathcal{F} = (\partial\mathcal{F}/\partial a)\delta a = 0$ and (from Eq. 12.3.1) $\partial\mathcal{F}/\partial a = bR(c) + \partial\Pi/\partial a = 0$

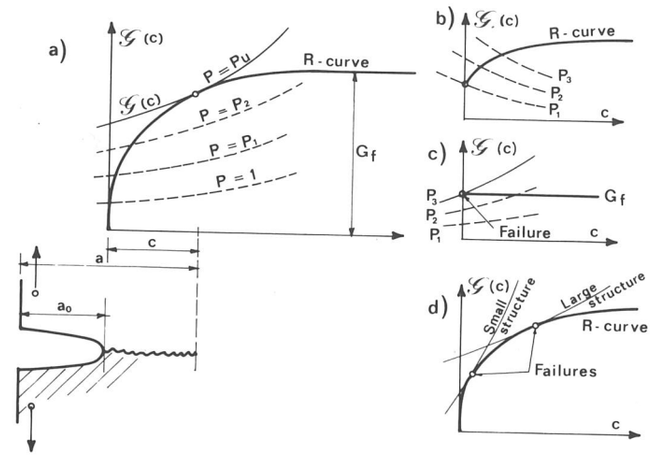

Figure 12.12 Curves of crack resistance to crack propagation (R curves) and of energy release rate: (a) $\mathcal{G}' > 0$; (b) $\mathcal{G}' < 0$; (c) R = const. = G_f; (d) critical stress for structures of different sizes. (*After Bažant and Cedolin, 1984.*)

(where $\partial\Pi/\partial a = \partial\Pi/\partial c$), it follows that a growing crack is in equilibrium if

$$\mathcal{G}(a) = R(c) \qquad \text{with } \mathcal{G}(a) = -\frac{\Pi'(a)}{b} \qquad c = a - a_0 \tag{12.3.2}$$

Here $\mathcal{G}(a)$ = energy release rate of the structure when the crack length is a, $\Pi'(a) = \partial\Pi(a)/\partial a$. In the special case of linear elastic fracture mechanics we have $R(c) = G_f$ = constant, and then Equation 12.3.2 becomes $-\partial\Pi/\partial a = bG_f$, as already indicated in Equation 12.1.1, where $\mathcal{G}$ = energy release rate of structure.

If $0 < \mathcal{G} < R(c)$, the crack can neither grow nor shorten, and so it is in equilibrium as a stationary crack.

If $\mathcal{G} = 0$, the crack can start closing near the tip, as the crack tip opening displacement δ_c is zero if $\mathcal{G} = 0$ or $K_I = 0$ (see Eqs. 12.1.5 and 12.2.4); this case represents the equilibrium state of crack shortening ($\delta a < 0$) because $\delta\mathcal{F} = (\partial\mathcal{F}/\partial a)\delta a = -b\mathcal{G}\delta a = 0$, that is, the energy required for crack closing is zero [as if $R(c) = 0$].

Under isentropic conditions, the only the change needed to be made in the foregoing equations is to replace $\mathcal{F}$ with total energy of the structure, $\mathcal{U}$. However, the values of $R(c)$ and G_f for isentropic conditions are different (larger) than for isothermal conditions.

Fracture Stability Criterion and Critical State

If the fracture equilibrium state is stable, the crack cannot propagate by itself, that is, without any change of loading (applied force or prescribed displacement). If the fracture equilibrium state is unstable, the crack will propagate by itself, without any change of applied load or boundary displacement. The fracture equilibrium state is stable if the second variation $\delta^2\mathcal{F}$ is positive (same as in Sec. 10.1). Since $\delta^2\mathcal{F} = \frac{1}{2}(\partial^2\mathcal{F}/\partial a^2)\delta a^2$ and $\partial^2\mathcal{F}/\partial a^2 = b(dR/dc) + \partial^2\Pi/\partial a^2$, we conclude that the equilibrium state of a growing crack satisfying Equation 12.3.2 is

Stable if	$R'(c) - \mathcal{G}'(a) > 0$		
Critical if	$R'(c) - \mathcal{G}'(a) = 0$	[if $\mathcal{G} = R(c)$]	(12.3.3)
Unstable if	$R'(c) - \mathcal{G}'(a) < 0$		

where $R'(c) = dR(c)/dc$ and $\mathcal{G}'(a) = \partial\mathcal{G}/\partial a = -(1/b)\partial^2\Pi(a)/\partial a^2$.

If $0 < \mathcal{G} < R(c)$, the crack is stable regardless of the sign of $R'(c) - \mathcal{G}'(a)$ because it can neither extend nor shorten.

If $\mathcal{G} = 0$ (or $K_I = 0$), we have an equilibrium state of crack shortening ($\delta a < 0$). It is

Stable if	$\mathcal{G}'(a) < 0$		
Critical if	$\mathcal{G}'(a) = 0$	(if $\mathcal{G} = 0$)	(12.3.4)
Unstable if	$\mathcal{G}'(a) > 0$		

If the equilibrium state of crack growth (or crack shortening) is unstable, the crack starts to propagate (or shorten) dynamically, and inertia forces must then be taken into account.

In the special case of linear elastic fracture mechanics, for which $R(c) = G_f$ = constant, we have $dR(c)/dc = 0$. In that case, conditions 12.3.3 for stability of a growing crack become identical to conditions 12.3.4.

For a structure with a single load P (or a system of loads with a single parameter P), Π is proportional to P^2. According to Equations 12.2.8, $\mathcal{G}(a) = P_u^2 g(\alpha)/Eb^2D$. For most structures and fracture specimens, $g(\alpha)$, and thus also $\mathcal{G}(a)$, are increasing functions. The plots of functions $\mathcal{G}(a)$ for a succession of increasing values $P = P_1, P_2, P_3, \ldots$ then look as shown by the dashed curve in Figure 12.12a (Bažant and Cedolin, 1984). According to Equation 12.3.2, the equilibrium states of crack propagation for various load values are the intersections of these dashed curves with the R curve. According to Equations 12.3.3, these equilibrium states are stable if $R'(c) > \mathcal{G}'(a)$ at the intersection point (Fig. 12.12a). As the load increases and the crack grows, the difference between the slopes $R'(c)$ and $\mathcal{G}'(a)$ gradually diminishes until, at a certain point, the slopes become equal (i.e. the curves become tangent); this is then the critical state, at which the load is maximum and the structure fails if the load is controlled. Beyond this point the crack extension is, under load control, unstable and occurs dynamically; the excess energy $\mathcal{G}(a) - R(c)$ goes into kinetic energy. The portion of the R curve before the critical state represents a stable crack growth (also called the "slow crack growth," to indicate the growth is not dynamic).

In the case that $g'(\alpha) < 0$ or $\mathcal{G}'(a) < 0$ (Fig. 12.12b), stability is guaranteed because $R'(c) > 0$. This case occurs for the double cantilever fracture specimen with a relatively short crack and for a rectangular specimen with a small centric crack loaded on the crack (as well as for specimens with chevron notches). For most other geometries, though, $g'(\alpha) > 0$ or $\mathcal{G}'(a) > 0$.

In the case that $R(c) = G_f$ = const. (Fig. 12.12c), stability under controlled load requires that $\mathcal{G}'(a) < 0$. So there can be no stable crack growth in linear elastic fracture mechanics except when $\mathcal{G}'(a) < 0$. Conversely, if a stable growth is observed and $\mathcal{G}'(a) > 0$, it means that the fracture law must be nonlinear.

Comparing structures that are geometrically similar (with similar notches) but of different sizes, the curves of $\mathcal{G}(c)$ are of similar shape (Fig. 12.12d), while the R curve remains the same. Consequently, the larger the structure, the larger is the crack length c at the maximum load (critical state under load control).

Determination of Geometry-Dependent *R* Curve from Size Effect Law

The foregoing quasi-elastic analysis of equilibrium propagation and stability can be carried out only if a realistic R curve is known. The R curve can be determined experimentally, but that is quite demanding and fraught with possible ambiguities. The main trouble, however, is that the experimentally measured R curve is valid only for specimens of similar geometry. For different geometries, the R curves are rather different (Bažant and Cedolin, 1984; Bažant, Kim, and Pfeiffer, 1986). This fact narrows the applicability of R curves, despite the attractive simplicity of this approach.

A different twist, however, has recently appeared, making the R curve approach much more versatile (Bažant and Kazemi, 1988). It has been found that the size effect law proposed by Bažant is much more broadly applicable than a

single R curve. One and the same size effect law, based on the same G_f and c_f (Eq. 12.2.11) applies for specimens of very different geometries while their R curves are very different (see fig. 8 in Bažant, Kim, and Pfeiffer, 1986). So the point is how to determine the R curve from the size effect law.

Consider now that the maximum load P_u has been measured for a set of geometrically similar specimens of different sizes D. For each size one has $\mathcal{G}(a) = P_u^2 g(\alpha)/Eb^2D$, where function $g(\alpha)$ is the same for all sizes D (Eqs. 12.2.8). On each curve $\mathcal{G}(a)$, there is normally one and only one point $a = a_1$ that represents the failure point (critical state). At this point, the $\mathcal{G}(a)$ curve must be tangent to the R curve. Consequently, the R curve is the envelope of the family of all the fracture equilibrium curves $\mathcal{G}(a)$ for different sizes, as shown in Figure 12.13.

To describe the envelope mathematically, we write the condition of equilibrium fracture propagation $f(c, D) = G(\alpha) - R(c) = 0$ where $\alpha = a/D = \alpha_0 + c/D$. If we slightly change size D to $D + \delta D$ but keep the geometric shape (that is, $\alpha_0 = \text{const.}$), failure (max P) occurs at a slightly different crack length $c + \delta c$. Since $f(c, D)$ must vanish both for D and $D + \delta D$, we must have $\partial f(c, D)/\partial D = 0$. Geometrically, the condition $\partial f(c, D)/\partial D = 0$ together with $f(c, D) = 0$ means that the R curve is the envelope of the family of fracture equilibrium curves $f(c, D) = 0$ for various D values (Bažant, Kim, and Pfeiffer, 1986). Because the $R(c)$ curve is a size-independent property, $\partial R(c)/\partial D = 0$. Therefore, the envelope condition is

$$\frac{\partial \mathcal{G}(\alpha)}{\partial D} = 0 \tag{12.3.5}$$

We have $P_u^2 = (\sigma_N bD/c_n)^2 = (Bf_u bD/c_n)^2/(1 + D/D_0)$ where $(Bf_u)^2 = c_n^2 E' G_f/D_0 g(\alpha_0)$ (according to Eq. 12.2.15). If we substitute this into $\mathcal{G}(\alpha) = P_u^2 g(\alpha)/E'b^2D$ (Eqs. 12.2.8), we obtain for the critical states

$$\mathcal{G}(\alpha) = G_f \frac{g(\alpha)}{g(\alpha_0)} \left(\frac{D}{D + D_0}\right) \tag{12.3.6}$$

Substituting this into the condition for the envelope, $\partial \mathcal{G}(\alpha)/\partial D = 0$ (Eq. 12.3.5),

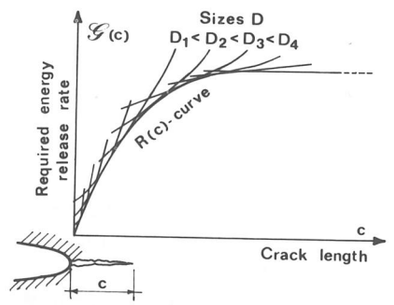

Figure 12.13 R curve as an envelope of fracture equilibrium curves. (*After Bažant, Kim, and Pfeiffer, 1986.*)

differentiating and noting that $\partial\alpha/\partial D = \partial\alpha_0/\partial D + \partial(c/D)/\partial D = -c/D^2 = -(\alpha - \alpha_0)/D$ (because $\alpha_0 = \text{const.}$ or $\partial\alpha_0/\partial D = 0$ for geometrically similar structures), we get

$$D + D_0 = \frac{D_0 g(\alpha)}{(\alpha - \alpha_0) g'(\alpha)} \tag{12.3.7}$$

Furthermore, substituting this, along with the relations $(\alpha - \alpha_0)D = c$ and $D_0 = c_f g'(\alpha_0)/g(\alpha_0)$ (from Eq. 12.2.16), into Equation 12.3.6, and setting $\mathcal{G}(\alpha) = R(c)$, we obtain the following result (Bažant and Kazemi, 1988, 1989):

$$R(c) = G_f \frac{g'(\alpha)}{g'(\alpha_0)} \left(\frac{c}{c_f}\right) \qquad \left(\alpha = \alpha_0 + \frac{c}{D}\right) \tag{12.3.8}$$

Equations 12.3.8 and 12.3.7 define the R curve parametrically. To calculate the R curve, we must first obtain G_f and D_0 from the size effect law (Eq. 12.2.11). Then we choose a series of α values. For each of them we evaluate D from Equation 12.3.7, get $c = (\alpha - \alpha_0)D$, and calculate R from Equation 12.3.8. When c is specified, then R needs to be solved by Newton iterations.

For different geometric shapes, functions $g(\alpha)$ are different, and so Equation 12.3.8 gives different R curves for different geometries. The R curves obtained in this manner, as well as the load-deflection diagrams calculated from such R curves, have been found to be in good agreement with various data on concrete and rocks, as well as aluminum alloys.

The foregoing derivation presumed the fracture process zone to remain attached to the tip of the notch or initial crack. This ceases to be true after passing the peak load; the fracture process zone becomes detached from the tip and subsequently its size remains approximately constant. Therefore it dissipates roughly the same amount of energy per unit crack extension. Consequently, the values of $\mathcal{G}$ after the peak load must be kept constant and equal to the value that $R(c)$ attained at the peak load (Bažant, Gettu, and Kazemi, 1989).

Determination of the R curve from the size effect does not work in all circumstances. It obviously fails when $g'(\alpha_0) = 0$, and does not work when $g'(\alpha_0) < 0$ or $g'(\alpha) \le 0$, because $g'(\alpha) > 0$ ($D_0 > 0$) was implied in the derivation of Equation 12.3.8. It also fails when $g'(\alpha_0)$ or $g'(\alpha)$ is too small, because of the scatter of test results. So this method must be limited to specimen geometries for which $g'(\alpha_0) > 0$ and $g'(\alpha) > 0$. This nevertheless comprises most practical situations.

Crack Propagation Direction

Another stability problem in crack propagation is that of propagation direction. Equilibrium modes of propagation can generally be found for many directions emanating from the tip of a crack or notch but only one will occur in reality. There exist several theories to decide the actual direction.

One theory assumes that the crack propagates in the direction normal to the maximum principal stress. If the trajectory is smoothly curved, this implies the propagation to occur in such a direction that the crack tip field would be of mode I. Another theory, due to Sih (1974), assumes the crack to propagate in the direction of minimum strain energy density. A third theory (Wu, 1978) holds that

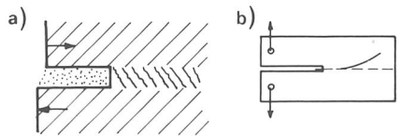

Figure 12.14 (a) Shear crack propagation in brittle materials; (b) crack kinking.

the crack should propagate in the direction that maximizes the energy release rate of the structure or specimen.

The last theory appears to be most reasonable since it in a certain sense maximizes the internally produced entropy increment at a deviation from the initial equilibrium state. The prediction of the last theory is often very close to that of the maximum principal stress theory. However, cracks in concrete have been observed to propagate under certain conditions in shear following the mode II direction (Bažant and Pfeiffer, 1987) or the mode III direction (Bažant, Prat, and Tabbara, 1989). The possibility of shear crack propagation seems to be typical of brittle materials with a coarse microstructure, in which the shear fracture propagates as a band of tensile (mode I) microcracks that are inclined with regard to the direction of propagation (Fig. 12.14a) and later coalesce into a continuous shear crack.

Kinking of Cracks and Three-Dimensional Instability of Front Edge

In some specimens with a symmetric (mode I) loading, the crack does not propagate straight, along the symmetry line, but deviates to the side. This phenomenon, called kinking, occurs, for example, in double cantilever specimens (Fig. 12.14b). Rice and Cotterel (1980) analyzed the kinking as a stability problem and showed that the straight-line propagation along the symmetry line is stable only if there is a normal compressive stress σ_x of sufficient magnitude in the propagation direction; see also Sumi, Nemat-Nasser, and Keer (1985).

Recently Rice also studied the condition when a propagating circular crack in an axisymmetric situation ceases to be circular. He showed that the crack front edge can develop a wavelike shape superimposed on the basic circular shape.

Problems

12.3.1 Supposing that $R(c) = G_f c/(k + c)$ where $k =$ constant, calculate the critical crack length and the stability region for the cracks in Figure 12.5a–h (Eqs. 12.1.13–12.1.22).

12.3.2 Do the same for $R(c) = G_f(1 - e^{-kc})$.

12.4 SNAPBACK INSTABILITY OF A CRACK AND LIGAMENT TEARING

In the preceding section, we formulated the stability criterion in terms of crack length increments that cause deviations from the fracture equilibrium state. From Section 10.1 we recall, however, that in the case of a single load or displacement

(or load parameter, displacement parameter) stability can be determined from the load-displacement diagram $P(u)$. With this aim in mind, we will now show how to calculate this diagram. Then we will apply the procedure to the terminal phase of the fracture process in which the distance between two crack tips or between a crack tip and a surface, called the ligament, is being reduced to zero.

General Procedure for Load-Displacement Relation at Growing Crack

Handbooks such as Tada, Paris, and Irwin (1985) or Murakami (1987) contain the solutions of many elastic crack problems. In most cases, though, they list only the stress intensity factor K_I (or K_{II}, K_{III}) as a function of the crack length a and the load P, but the displacement is not given because it does not directly figure in many analytical methods of elastic analysis. Yet, if the entire structure is elastic, u can be calculated from $K_I(a)$ quite easily as follows (Bažant, 1987b).

Consider a body with a single load P (or a single loading parameter P). Instead of the actual process of equilibrium crack growth at $\mathcal{G} = R(c)$, the current state with load P, load-point displacement u, and crack length a may be imagined to be reached by two other loading processes at which mechanical equilibrium is maintained [but the condition of $\mathcal{G} = R(c)$ is violated].

Process I. Load P is applied first on an uncracked specimen (Fig. 12.15a) and then, while P is kept constant, a crack grows from length 0 to length a (Fig. 12.15b), which causes additional displacement u_f. The energy release rate is $\mathcal{G} = K_I^2/E'$ (Eq. 12.1.8) where $K_I = Pk(\alpha)/b\sqrt{D}$ for two-dimensional similarity (2D, Eqs. 12.2.8) or $K_I = Pk(\alpha)D^{-3/2}$ for three-dimensional similarity (3D, Eqs. 12.2.9), and $E' = E/(1 - \nu^2)$ for plane strain, $E' = E$ for plane stress and for 3D. The energy dissipated by the crack tip is

For 2D:

$$W_f = b\int \mathcal{G}D\, d\alpha = \frac{P^2\phi(\alpha)}{E'b} \qquad \phi(\alpha) = \int_0^\alpha [k(\alpha')]^2\, d\alpha' \qquad (12.4.1a)$$

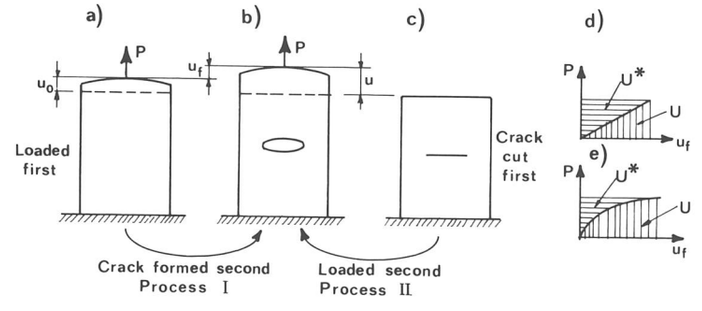

Figure 12,15 (a, b, c) Two loading and cracking sequences leading to the same final state of an elastic solid; strain energy and complementary strain energy for (d) linear and (e) nonlinear elasticity.

For axisymmetric or other 3D situations:

$$W_f = \int p(\alpha) D \mathcal{G} D \, d\alpha = \frac{P^2 \psi(\alpha)}{E'D} \qquad \psi(\alpha) = \int_0^\alpha p(\alpha')[k(\alpha')]^2 \, d\alpha' \quad (12.4.1b)$$

in which $D\,d\alpha = da$ and $p(\alpha)D$ = perimeter of the crack front edge in three-dimensional situations. For example, $p(\alpha) = 2\pi\alpha$ for a circular crack of radius a in a bar of diameter D.

The change of potential energy needed to produce the crack is $\Delta\mathcal{F} = \Pi + W_f$ where $\Pi = U - W = U - \int P\,du_f = U - Pu_f$ = potential-energy change without regard to fracture, W = work of load, U = strain energy change (at constant temperature), and $\Delta\mathcal{F}$ represents the Helmholtz free energy of the system (cf. Eq. 12.5.1). Since there is no external energy input other than load P, we have $\Delta\mathcal{F} = 0$, from which

$$W_f = Pu_f - U \quad (12.4.2)$$

(alternatively we could have written this relation directly on the basis of energy conservation requirements). Now we notice that the expression $U^* = Pu_f - U$ coincides with the definition of the complementary strain energy (Fig. 12.15d). Moreover, for constant load ($dP = 0$), the complementary energy of the structure-load system is $\Pi_f^* = U^* - W^* = U^*$ because $W^* = \int u_f\,dP = 0$ (complementary work of the load at $dP = 0$). So we conclude that

$$\Pi_f^* = W_f \quad (12.4.3)$$

The total complementary energy of the cracked structure is $\Pi^* = \Pi_0^* + \Pi_f^*$ where $\Pi_0^* = \Pi_0^*(P)$ = complementary strain energy of the structure if there is no crack.

Process II. The crack of length a is imagined to be cut prior to loading (in an unstressed body, Fig. 12.15c), and then the load is increased from 0 to P while the crack length a is kept constant. Because the body is elastic, the principle of conservation of energy must apply, and so the complementary energy at the end of this process must be the same, that is, $\Pi^* = \Pi_0^* + \Pi_f^*$ where Π_0^* = change of complementary energy calculated for a body with no crack.

Process II has the advantage that we may apply Castigliano's theorem to calculate the displacements; $u = \partial\Pi^*/\partial P$. Therefore,

$$u(P) = \frac{\partial\Pi_0^*}{\partial P} + \frac{\partial\Pi_f^*}{\partial P} = u_0(P) + u_f(P) \quad (12.4.4)$$

in which $u_0(P) = \partial\Pi_0^*(P)/\partial P$ = displacement calculated for a body with no crack (Fig. 12.15a), and $u_f(P) = \partial\Pi_f^*(P)$ where $u_f(P)$ represents the additional load-point displacement due to crack, which must be equal to the displacement caused in process I by creating the entire crack at constant load P (Fig. 12.15b). The additivity of the displacement due to crack, stated by Equation 12.4.4, is a basic simple principle for calculating deformations of cracked elastic bodies.

According to $u_f = \partial\Pi_f^*/\partial P$, Equations 12.4.1 yields

For 2D:

$$u_f = \frac{\partial\Pi_f^*}{\partial P} = \frac{2P}{E'b}\phi(\alpha) \quad (12.4.5a)$$

For axisymmetric or other 3D situations:

$$u_f = \frac{\partial\Pi_f^*}{\partial P} = \frac{2P}{E'D}\psi(\alpha) \quad (12.4.5b)$$

Now consider the actual loading process, in which the crack grows gradually as the load is increased. During the actual crack growth (in contrast to processes I and II) we must have $\mathcal{G} = R(c)$ or $K_I = K_I^R(c)$ satisfied all the time; $K_I^R(c) = [E'R(c)]^{1/2}$ = critical stress intensity factor depending on the crack extension $c = \alpha D - a_0$ according to the R curve (which must be calculated in advance as we showed in Sec. 12.3). Consequently, from Equations 12.2.8 and 12.2.9,

For 2D:

$$P = \left[\frac{E'b^2D}{g(\alpha)}R(c)\right]^{1/2} = \frac{b\sqrt{D}}{k(\alpha)}K_I^R(c) \quad (12.4.6a)$$

For axisymmetric or other 3D situations:

$$P = \left[\frac{E'D^3}{g(\alpha)}R(c)\right]^{1/2} = \frac{D^{3/2}}{k(\alpha)}K_I^R(c) \quad (12.4.6b)$$

Analogous equations, in which K_I^R is replaced by K_{II}^R or K_{III}^R, apply to mode II or mode III fracture.

Equations 12.4.5a, b and 12.4.6a, b describe the load-deflection curve $P(u)$ at advancing crack in a parametric way, with a as the parameter. For any value of a, one may calculate P from Equations 12.4.6a, b and u_f from Equations 12.4.5a, b. Adding $u_0(P)$, one obtains u.

A similar derivation can be made when the boundary conditions consist of a specified remote stress σ_∞ instead of load P.

Snapback Instability at Crack Coalescence in Two Dimensions

To demonstrate stability analysis based on the foregoing procedure, consider a periodic array of collinear cracks of length $2a$ and center-to-center spacing D in an infinite space subjected at infinity to tensile stress σ normal to the cracks (Ortiz, 1987; Horii, Hasegawa, and Nishino, 1987; Bažant, 1987b) (Fig. 12.16a). This problem is of interest for micromechanics of the fracture process zone in brittle heterogeneous materials, such as concrete or modern toughened ceramics. According to Equation 12.1.19 (Tada, Paris, and Irwin, 1985) we have

$$\frac{1}{b}\frac{\partial\Pi_f^*}{\partial a} = 2\mathcal{G} = \frac{2K_I^2}{E'} = \frac{2\sigma^2}{E'}D\tan\frac{\pi a}{D} \quad (12.4.7)$$

with $E' = E/(1-\nu^2)$, for both crack tips combined. By integration, the strain energy released by symmetric crack formation is

$$\Pi_f^* = -\frac{2\sigma^2D^2b}{\pi E'}\ln\left(\cos\frac{\pi a}{D}\right) \quad (12.4.8)$$

The relative displacement due to cracks, measured between two planes remote

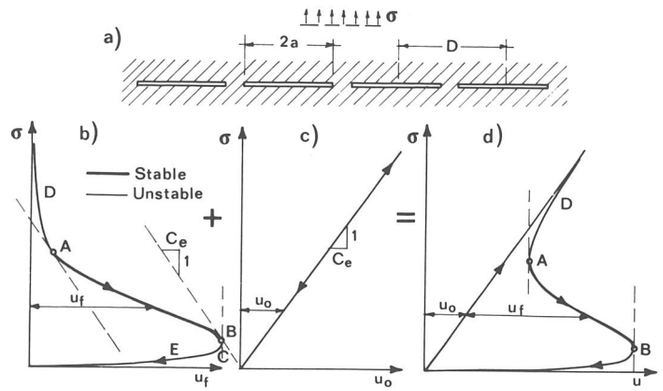

Figure 12.16 (a) Array of collinear cracks, (b, c, d) determination of snapback instability and graphical construction of stress–displacement diagram.

from the crack plane, is (by Castigliano's theorem)

$$u_f = \frac{\partial \Pi_f^*}{\partial P} = \frac{1}{bD}\frac{\partial \Pi_f^*}{\partial \sigma} = -\frac{4\sigma D}{\pi E'} \ln\left(\cos\frac{\pi a}{D}\right) \tag{12.4.9}$$

where $P = \sigma Db$ = force per crack. Although linear elastic fracture mechanics does not apply to macroscopic fracture of concrete or toughened ceramics, it may probably be assumed to apply to microcracks, and so we may use $R(c) = G_f =$ const. Setting $\mathcal{G} = R(c)$, we also have

$$\sigma = \left(\frac{E'G_f}{D \tan(\pi a/D)}\right)^{1/2} \tag{12.4.10}$$

Equations 12.4.9 and 12.4.10 define the relation $\sigma(u_f)$ in a parametric way, with a as a parameter. We may assume the R curve in the form $R(a) = G_f[1-(1-a/c_m)^n]$ for $a \le c_m$ and $R(a) = G_f$ for $a \ge c_m$ where G_f, c_m, and n are material constants and c_m has the dimension of length (Bažant, Kim, and Pfeiffer, 1986). Then, if we choose various values of a, we can calculate the corresponding values of $\sigma(a)$ and $u_f(a)$. The resulting curve $\sigma(u_f)$ is plotted in Figure 12.16b (for $n = 2.8$, $c_m = 0.1$ in.). An interesting property is that, after a maximum displacement u_f, this curve exhibits snapback.

The stress σ, in reality, is not applied or controlled at infinity but at some remote planes at distance L, parallel to the cracks. To judge stability one needs the total displacement $u(\sigma) = u_f(\sigma) + u_0(\sigma)$ where $u_0(\sigma) = C_e\sigma$, $C_e = L/E' =$ relative displacements between these planes if no cracks existed. Based on this relation, one may construct the $u(\sigma)$ diagram graphically by adding the abscissas for the same value of σ as shown in Figure 12.16b, c, d. Clearly, the resulting diagram $\sigma(u)$ (Fig. 12.16d) also exhibits snapback.

Since the diagram $\sigma(u)$ is descending, the states of growing cracks cannot be stable under load control. They can be stable only if displacement u is controlled, but never after the snapback point. The stability condition is $du/dP < 0$ (see Sec. 10.1). The critical state is obtained for $du/dP = 0$, which means drawing vertical tangents as shown in Figure 12.16d. Stability (under displacement control) exists

only between the tangent points. Since $u = u_f + C_e\sigma$, one finds that the state of growing cracks under displacement control is

$$\begin{aligned} &\text{Stable if} && \frac{du_f}{d\sigma} < -C_e \\ &\text{Critical if} && \frac{du_f}{d\sigma} = -C_e \\ &\text{Unstable if} && \frac{du_f}{d\sigma} > -C_e \end{aligned} \tag{12.4.11}$$

This stability condition is illustrated in Figure 12.16b where dashed straight lines of slope $-1/C_e$ are drawn as tangents to the calculated $u_f(\sigma)$ diagram. There are two tangent points A and B representing the critical states. Between these critical states (segment AB) the growing crack is stable, and the remaining points on the $u_f(\sigma)$ curve (branches DA and BE) are unstable. The shorter length L is, the steeper is the slope $-1/C_e$, which causes the stability region to increase. However, no matter how steep this slope is, the critical state cannot be pushed beyond point C with a vertical tangent.

Snapback Instability at Tearing of Circular Ligament

For micromechanics of the fracture process zone in concrete or toughened ceramics, a more realistic model for the terminal process of ligament tearing is shrinking circular ligaments of spacing D, connecting two elastic half-spaces in three dimensions. As stated in Equation 12.1.22, $K_I = \frac{1}{2}P(\pi r^3)^{-1/2}$ (Tada, Paris, and Irwin, 1985) where r = ligament radius and P = transverse force transmitted by one ligament. From this, $-\partial\Pi_f^*/\partial r = \partial\Pi_f^*/\partial a = 2\pi r\mathcal{G} = 2\pi r K_I^2/E' = P^2/2E'r^2$ where $E' = E/(1-\nu^2)$. By integration,

$$\Pi_f^* = \frac{P^2}{2E'}\left(\frac{1}{r} - \frac{\kappa}{D}\right) \qquad r = \frac{D}{2} - a \tag{12.4.12}$$

where κ = integration constant. By Castigliano's second theorem,

$$u_f = \frac{\partial \Pi_f^*}{\partial P} = \frac{P}{E'}\left(\frac{1}{r} - \frac{\kappa}{D}\right) \tag{12.4.13}$$

Also, setting $\mathcal{G} = R(c) = G_f$ we obtain $r = (P^2/4\pi E'G_f)^{1/3}$, and Equation 12.4.13 then becomes

$$u_f = \frac{P}{E'}\left[\left(\frac{4\pi E'G_f}{P^2}\right)^{1/3} - \frac{\kappa}{D}\right] \tag{12.4.14}$$

Constant κ can be determined from some known state at finite r. Requiring Equation 12.4.14 to pass through the snapback point obtained from a more realistic model, Bažant (1987b) found $\kappa = 2.299$.

The plot of Equation 12.4.14 is shown in Figure 12.17b as the lower dashed curve. Obviously, Equation 12.4.14 represents snapback, and we could repeat a similar discussion as before. Figure 12.17a, b also exhibits the solutions obtained by Bažant (1987b) for the two idealized three-dimensional situations shown,

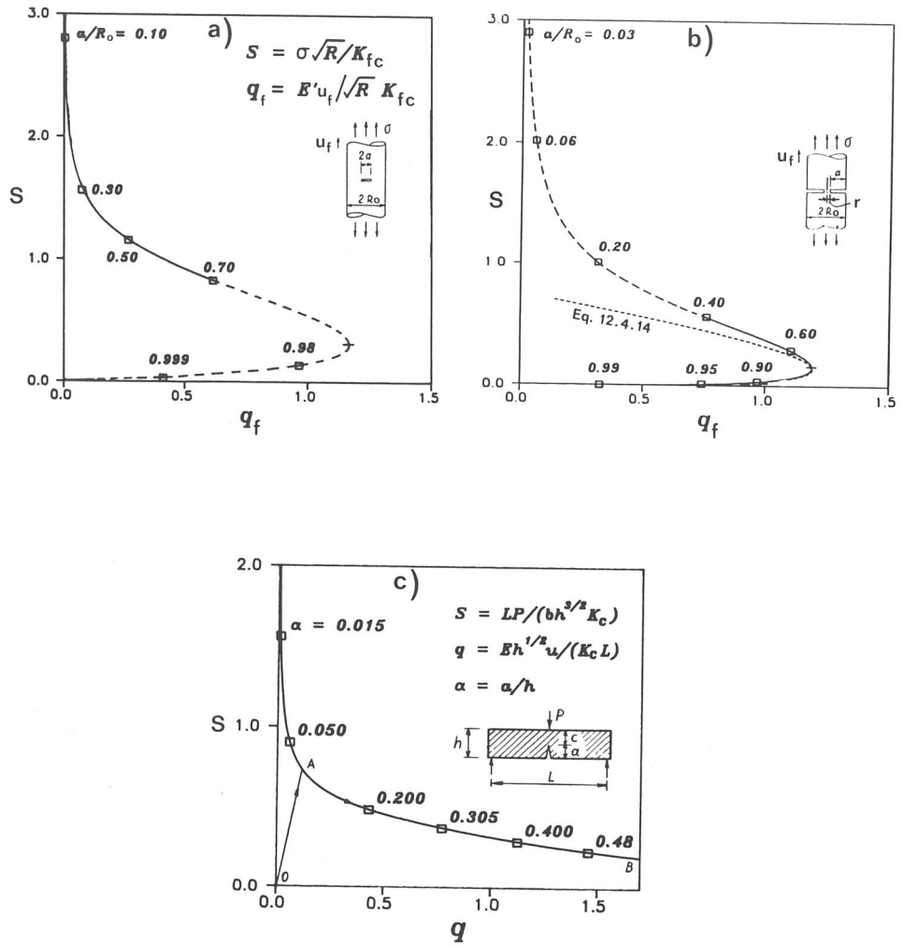

Figure 12.17 Stress–displacement diagrams for (a) circular (penny-shaped) crack, (b) circular ligament, (c) three-point bent beam. (*After Bažant, 1987b.*)

which model the evolution of fracture in the process zone from small circular cracks to small circular ligaments.

With regard to the stress–displacement (or stress–strain) relation for the fracture process zone, the foregoing results suggest that it should be considered to possess a certain maximum displacement (or strain). Conceivably, though, various other inelastic phenomena could spoil this picture; see the discussion in Bažant (1987b).

General Condition for Snapback at Ligament Tearing

Does the snapback always take place in the terminal phase of fracture? It does not. For example, using Srawley's expression for K_I, Bažant (1987b) used the technique we just demonstrated to calculate the $P(u_f)$ diagram for a three-point

bend fracture specimen; see Figure 12.17c; it exhibits no snapback instability. So what is the property that causes snapback?

Let us consider the ligament size to be infinitely small compared to any cross-section dimension of the structure. We assume the subsequent ligament shapes to remain similar as the ligament shrinks. Let P and M be the internal force of any direction and the internal moment about any axis transmitted across the ligament (Fig. 12.18). (The special cases of P include a normal force or a shear force, and of M a bending moment or a twisting moment.) According to Saint-Venant's principle, P or M can produce significant stresses and significant strain energy density only in a three-dimensional region whose size (L_1 and L_2 in Fig. 12.18) is of the same order of magnitude as the ligament size $2r$. The strain energy produced in this region by P or M is

$$\Pi_1^* = \frac{P^2}{2EA}k_1 r = \frac{P^2}{2Ek_3 r} \qquad \Pi_2^* = \frac{M^2}{2EI}k_2 r = \frac{M^2}{2Ek_4 r^3} \tag{12.4.15}$$

where $A = k_5 r^2$ = cross-section area of the ligament, $I = k_6 r^4$ = moment of inertia of the cross section of the ligament, and $k_1, k_2, \ldots, k_6$ = constants. The remote displacement u_f and rotation θ associated with P and M, respectively, are

$$u_f = \frac{\partial \Pi_1^*}{\partial P} = \frac{P}{Ek_3 r} \qquad \theta = \frac{\partial \Pi_2^*}{\partial M} = \frac{M}{Ek_4 r^3} \tag{12.4.16}$$

The energy release rates due to P and M per unit circumference of the ligament cross section are

$$\mathcal{G}_1 = -\frac{1}{k_7 r}\frac{\partial \Pi_1^*}{\partial r} = \frac{P^2}{2Ek_3 k_7 r^3} \qquad \mathcal{G}_2 = -\frac{1}{k_8 r}\frac{\partial \Pi_2^*}{\partial r} = \frac{3M^2}{2Ek_4 k_8 r^5} \tag{12.4.17}$$

Setting $\mathcal{G}_1 = G_f$ or $\mathcal{G}_2 = G_f$, we have

$$\text{For } P: \quad r = \left(\frac{P^2}{2Ek_3 k_7 G_f}\right)^{1/3} \qquad \text{For } M: \quad r = \left(\frac{3M^2}{2Ek_4 k_8 G_f}\right)^{1/5} \tag{12.4.18}$$

Substituting this into Equations 12.4.16 we get, for very small ligament size r, the

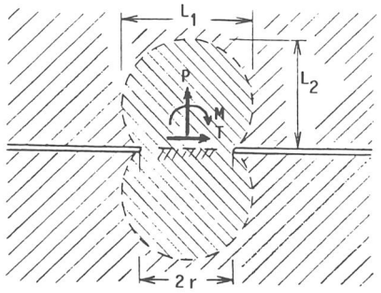

Figure 12.18 Tearing of ligament joining two half-spaces or half-planes. (*After Bažant, 1987b.*)

asymptotic approximations:

$$\begin{aligned} &\text{For } P: && v = c_1 P^{1/3} \\ &\text{For } M: && \theta = c_2 M^{-1/5} \end{aligned} \tag{12.4.19}$$

where c_1, c_2 = constants. Note that Equation 12.4.19 for P agrees with the asymptotic form of Equation 12.4.14, which is $u_f^3 = 4\pi G_f P/E'^2$ for $P \to 0$.

From Equations 12.4.19 we conclude that if the ligament is loaded by a force, the curve $u_f(P)$ must return to the origin ($u_f = P = 0$) as $P \to 0$ ($r \to 0$). This implies that there must be snapback at some finite P value.

On the other hand, if the ligament is loaded by a moment, the curve $\theta(M)$ tends to infinity as $M \to 0$ ($r \to 0$). So there can be no snapback.

For two-dimensional problems a similar asymptotic analysis is possible, but only for the moment loading. We have $I = k_6 b r^3$ where b = thickness of the body, and instead of Equations 12.4.15 to 12.4.17 we obtain

$$\Pi_2^* = \frac{M^2}{2EI} k_2 r = \frac{M^2}{2Ek_4 b r^2} \tag{12.4.20}$$

$$\theta = \frac{\partial \Pi_2^*}{\partial M} = \frac{M}{Ek_4 b r^2} \tag{12.4.21}$$

$$\mathcal{G}_2 = -\frac{\partial \Pi_2^*}{b\,\partial r} = \frac{M^2}{Ek_4 b^2 r^3} \tag{12.4.22}$$

Setting $\mathcal{G} = G_f$, we have $r = (M^2/G_f E k_4 b^2)^{1/3}$, and substituting this into Equation 12.4.21 we get, for small r,

$$\theta = c_2 M^{-1/3} \tag{12.4.23}$$

So for moment loading in two dimensions there cannot be any snapback either.

For two-dimensional problems in which the ligament is loaded by a force, the foregoing approach fails because, as it turns out, the curve $u_f(P)$ is not of a power type as $P \to 0$. For a sufficiently short ligament, the stress field must be the same as that near a ligament joining two elastic half-planes. For that problem it is known that $K_I = (P/b)(\pi r)^{-1/2}$ where P = normal (centric) force and r = half-length of the ligament (Fig. 12.18). Therefore $-\partial \Pi_f^*/\partial r = b\mathcal{G} = bK_I^2 E' = P^2/\pi E' b r$, and by integration the total strain energy release is

$$\Pi_f^* = -\frac{P^2}{\pi E' b} \ln \frac{r}{r_0} \tag{11.4.24}$$

where r_0 = integration constant. Furthermore,

$$u_f = \frac{\partial \Pi_f^*}{\partial P} = -\frac{2P}{\pi E' b} \ln \frac{r}{r_0} \tag{12.4.25}$$

Setting $K_I = K_{Ic}$ = critical value of K_I, we also get $r = P^2/\pi b^2 K_{Ic}^2$, and substitution into Equation 12.4.25 yields

$$u_f = -\frac{2P}{\pi E' b} \ln \frac{P^2}{\pi b^2 K_I^{R^2} r_0} \tag{12.4.26}$$

The curve $u_f(P)$ described by this equation is not of a power type, which explains why the type of approach used in Equations 12.4.15 to 12.4.23 would fail.

The curve $u_f(P)$ given by Equation 12.4.26 obviously exhibits a snapback since, for $P \to 0$, $\lim u_f = 0$. The critical state is characterized by the condition $\partial u_f/\partial P = 0$. u_f yields for the snapback instability the critical load $P_{cr} = K_I^R b\sqrt{\pi r_0}/7.389$; max u_f follows from Equation 12.4.26.

Note: Coalescence of adjacent circular voids in a plastic material is a related stability problem. It is of interest for micromechanics of fracture propagation in metals.

Alternative Calculation of Displacement from Compliance Variation

Instead of using Castigliano's theorem and complementary energy, we can alternatively calculate the load-point displacement u by integrating the changes of compliance C. We again consider a process in which load P is applied first on an uncracked structure and then, while P is kept constant, the crack grows from length 0 to length a (see process I in Fig. 12.15a, b). According to Equation 12.1.1, the energy release rate during this process is, for 2D, $\mathcal{G} = (\partial \Pi^*/\partial a)/b = b^{-1} d[\frac{1}{2} C(a) P^2]/da = (P^2/2b)\, dC(a)/da$ (Eq. 12.1.12), and for axisymmetric or other 3D situations $\mathcal{G} = (\partial \Pi^*/\partial a)/p(\alpha) D$. Substituting $\mathcal{G} = K_I^2/E'$, we obtain

For 2D:

$$\frac{dC(a)}{da} = \frac{2bK_I^2(a)}{P^2 E'} = \frac{2[k(\alpha)]^2}{bDE'} \tag{12.4.27a}$$

For axisymmetric or other 3D situations:

$$\frac{dC(a)}{da} = \frac{2p(\alpha) D K_I^2(a)}{P^2 E'} = \frac{2p(\alpha)[k(\alpha)]^2}{D^2 E'} \tag{12.4.27b}$$

where $\alpha = a/D$. The initial value of C for $a = 0$ is the compliance C_0 of the same structure with no crack. Thus, setting $da = D\, d\alpha$ and integrating Equations 12.4.1a, b at P = const. from $C(0) = C_0$ to $C(a)$, we obtain

$$C(a) = C_0 + C_f(a) \tag{12.4.28}$$

where

For 2D:

$$C_f(a) = \frac{2\phi(\alpha)}{bE'} \qquad \phi(\alpha) = \int_0^\alpha [k(\alpha')]^2\, d\alpha' \tag{12.4.29a}$$

For axisymmetric or other 3D situations:

$$C_f(a) = \frac{2\psi(\alpha)}{DE'} \qquad \psi(\alpha) = \int_0^\alpha p(\alpha')[k(\alpha')]^2\, d\alpha' \tag{12.4.29b}$$

$C_f(a)$ represents the additional compliance due to the crack. Equation 12.4.28 proves that the compliance of the uncracked structure and the compliance due to the crack are additive. According to Equation 12.4.28, the load-point displacement is $u(P) = u_0(P) + u_f(P)$ where $u(P) = C_0 P$ and $u_f(P) = C_f(a)P$. Substituting Equations 12.4.29a, b, we get for u_f the same expression as in Equations 12.4.5a, b.